

Thermodynamic Model for the Solubility of Cr(OH)₃(am) in Concentrated NaOH and NaOH–NaNO₃ Solutions¹

Dhanpat Rai,² Nancy J. Hess,² Linfeng Rao,³ Zhicheng Zhang,³
Andrew R. Felmy,² Dean A. Moore,² Sue B. Clark,⁴
and Gregg J. Lumetta²

Received February 9, 2001; revised January 31, 2002

The main objective of this study was to develop a thermodynamic model for predicting Cr(III) behavior in concentrated NaOH and in mixed NaOH–NaNO₃ solutions for application to developing effective caustic leaching strategies for high-level nuclear waste sludges. To meet this objective, the solubility of Cr(OH)₃(am) was measured in 0.003 to 10.5 *m* NaOH, 3.0 *m* NaOH with NaNO₃ varying from 0.1 to 7.5 *m*, and 4.6 *m* NaNO₃ with NaOH varying from 0.1 to 3.5 *m* at room temperature (22 ± 2°C). A combination of techniques, X-ray absorption spectroscopy (XAS) and absorptive stripping voltammetry analyses, were used to determine the oxidation state and nature of aqueous Cr. A thermodynamic model, based on the Pitzer equations, was developed from the solubility measurements to account for dramatic increases in aqueous Cr with increases in NaOH concentration. The model includes only two aqueous Cr species, Cr(OH)₄[−] and Cr₂O₂(OH)₄^{2−} (although the possible presence of a small percentage of higher oligomers at >5.0 *m* NaOH cannot be discounted) and their ion–interaction parameters with Na⁺. The logarithms of the equilibrium constants for the reactions involving Cr(OH)₄[−] [Cr(OH)₃(am) + OH[−] ⇌ Cr(OH)₄[−]] and Cr₂O₂(OH)₄^{2−} [2Cr(OH)₃(am) + 2OH[−] ⇌ Cr₂O₂(OH)₄^{2−} + 2H₂O] were determined to be −4.36 ± 0.24 and −5.24 ± 0.24, respectively. This model was further tested and provided close agreement between the observed Cr concentrations in equilibrium

¹Notice: This manuscript has been authored by Battelle Memorial Institute, Pacific Northwest Division, under Contract No. DE-AC06-76RL0 1830 with the U.S. Department of Energy. The publisher, by accepting the article for publication, acknowledges that the United States Government retains a nonexclusive, paid up, irrevocable, world-wide license to publish or reproduce the published of this manuscript, or allow others to do so, for United States Government purposes.

²Pacific Northwest National Laboratory Richland, Washington 99352; email: dhan.raai@pnl.gov

³Lawrence Berkeley National Laboratory, Berkeley, California 94720.

⁴Washington State University, Pullman, Washington 99164-4630.

with $\text{Cr}(\text{OH})_3(\text{am})$ in mixed NaOH – NaNO_3 solutions and with high-level tank sludges leached with and primarily containing NaOH as the major electrolyte.

KEY WORDS: Thermodynamics; $\text{Cr}(\text{OH})_3(\text{am})$; solubility; hydrolysis constants; polynuclear species; $\text{Cr}_2\text{O}_2(\text{OH})_4^{2-}$; $\text{Cr}(\text{OH})_4^-$; ion–interaction parameters.

1. INTRODUCTION

The safe disposal of high-level nuclear wastes existing at United States Department of Energy (DOE) sites requires advanced technologies, such as vitrification of these wastes into glass to immobilize the radioactive materials. Unfortunately, the presence of certain components, particularly chromium, in the wastes presents serious problems to the vitrification process and greatly influences the volume and quality of the glass to be produced. For example, during vitrification, under the proposed operating temperature of the glass melter (1050–1150°C), even relatively small amounts of Cr can result in the formation of refractory spinel crystalline solid phases. The formation and settling of crystallites during the vitrification process can adversely affect melter performance.⁽¹⁾ Consequently, the allowable limits for Cr in the melter feed must be low (0.34 wt.%).⁽²⁾ Because Cr content in tanks can be considerably higher than 0.34 wt.% and, in some tanks, is known to reach as high as 24 wt.% of water-insoluble solids,⁽³⁾ Cr is considered an important constituent in defining the total volume of high-level waste glass to be produced from DOE's Hanford tank wastes. It is, therefore, essential to develop pretreatment technologies [e.g., caustic leaching^(4–6)] to remove Cr from the tank sludges before vitrification.

Approximately 785 metric tons (MT) of Cr are present in the high-level nuclear waste storage tanks at Hanford.⁽⁷⁾ Recent spectroscopic investigations⁽⁸⁾ of untreated tank sludges indicate that Cr is present in widely varying proportions of Cr(III) and Cr(VI) that, in general, can be correlated to the processes (bis-muth phosphate, BiPO_4 ; tributyl phosphate, TBP; reduction oxidation, REDOX; plutonium-uranium extraction, PUREX) used to extract Pu from spent fuel.⁽⁹⁾ In the BiPO_4 and REDOX processes, Cr was added as $\text{Na}_2\text{Cr}_2\text{O}_7$ to oxidize Pu. In the REDOX process, appreciable amounts of Cr were added as $\text{Cr}(\text{NO}_3)_3$ hydrate to aid in the precipitation of MnO_2 . As a result, the bulk of the Cr in the waste inventory is associated with REDOX process waste.⁽¹⁰⁾ In addition, approximately 68 MT of Cr resulted from the corrosion of steel transfer lines and underground tanks.⁽⁷⁾ The facts that (1) the major proportion of Cr in the Hanford tanks exists in the solid matrix^(5,6) and that (2) most Cr(VI) solids⁽¹¹⁾ are very soluble suggest that the dominant oxidation state of Cr in most high-level nuclear waste storage tanks at Hanford must be Cr(III). This is consistent with the observations^(5,6,12) that the high-level tank sludges contain several Cr(III) solid phases, including Cr(III) hydroxide or hydrous oxides associated with Fe(III)/Al(III) hydroxides (e.g., CrOOH ,

Al/Cr(OH)₃(am), AlO₂/Cr(OH)₃(am), FeCr₂O₄, and Fe(Cr,Fe)₂O₄). Currently, several pretreatment strategies for removing Cr from the sludges are being developed, including caustic leaching with NaOH, leaching with NaOH in the presence of selected oxidants, and leaching with NaOH at elevated temperatures. Because caustic leaching is the baseline method for pretreating Hanford tank sludges, fundamental knowledge of the solubility of Cr(III) phases in aqueous NaOH is essential to full understanding of the process chemistry. The focus of this study, therefore, is on the speciation and solubility reactions of Cr(III), which are important in chemical conditions encountered in high-level nuclear waste storage tanks at Hanford.

The efficiency of Cr(III) removal in caustic leaching will depend on the nature of the solid phases and on the aqueous speciation of Cr in highly concentrated NaOH and in mixtures of NaOH and other important electrolytes, such as NaNO₃, which are also known to be present in the wastes. A literature survey indicates only a limited number of experimental studies that address the aqueous speciation and solubility of Cr(OH)₃(s) in basic solutions.⁽¹³⁻¹⁶⁾ Despite the fact that data are limited, there is quite good agreement, with the exception of data reported by Fricke and Windhausen,⁽¹³⁾ among the three other studies. For example, the minimum solubilities of amorphous Cr(III) hydroxide reported by Rai *et al.*⁽¹⁴⁾ and von Meyenburg *et al.*⁽¹⁶⁾ are very similar ($10^{-6.84}$ and $10^{-7.0}$ M, respectively) and the logarithm (base 10) of the equilibrium constant for the reaction $[\text{Cr}^{3+} + 4\text{H}_2\text{O} \rightleftharpoons \text{Cr}(\text{OH})_4^- + 4\text{H}^+]$ estimated from Rai *et al.*⁽¹⁴⁾ and that reported by Ziemniak *et al.*⁽¹⁵⁾ are very similar (< -27.65 and -27.38). Fricke and Windhausen⁽¹³⁾ studied the solubility of Cr(OH)₃(am) in NaOH concentrations ranging from 0.9 to 17.4 M. Their observed solubility in about 1.0 M NaOH is several orders of magnitude higher than that observed by Rai *et al.*⁽¹⁴⁾ The specific reasons for these differences are not known. However, we surmise that the differences may result from inadequate control or lack of control of important experimental variables (*e.g.*, filtration and the gaseous atmosphere) in the study conducted by Fricke and Windhausen.⁽¹³⁾ The currently available thermodynamic data^(14,15,17) are useful only for possibly predicting Cr(III) concentrations in systems where ionic strengths and base concentrations are relatively low. However, these data are not directly applicable to predicting Cr concentrations in high-level nuclear wastes stored in tanks or processing of these wastes where the Cr chemistry is complicated by the presence of highly concentrated base and bulk electrolytes, such as NaNO₃.

Our objectives for these studies, therefore, were to determine the solubility of Cr(OH)₃(am) as functions of NaOH and NaNO₃ concentrations, to develop a thermodynamic model to predict the solubility behavior of Cr(OH)₃(am) in highly alkaline/mixed electrolyte solutions, and to provide a basis for the development of sludge-leaching strategies for Cr removal. To meet these objectives, we (1) determined the solubility of Cr(OH)₃(am) in NaOH solutions

extending to 10.5 *m*, in 3.0 *m* NaOH solutions with NaNO₃ concentrations from 0.1 to 7.5 *m*, and in 4.6 *m* NaNO₃ solutions with NaOH concentrations from 0.1 to 3.5 *m*; (2) developed a thermodynamic model based on Pitzer's specific ion interaction approach; and (3) tested this model against empirical data from the washing of high-level nuclear waste tank sludges with caustic solutions.⁽⁴⁻⁶⁾ Close agreement between the observed and model-predicted Cr concentrations in caustic leachates of sludges from 14 different tanks, especially for the second caustic leach, confirm the reliability and utility of the model developed in this study.

2. EXPERIMENTAL PROCEDURES

The experimental procedures used in this study followed as closely as possible the procedure of Rai *et al.*,⁽¹⁴⁾ who examined the solubility of Cr(OH)₃(am) in dilute sodium perchlorate solutions. All experiments were conducted in controlled-atmosphere chambers containing an inert gas at room temperature (22 ± 2°C). A 1.0 *M* Cr(III) stock solution was prepared from reagent grade Cr(NO₃)₃ · 9H₂O in 0.1 *M* HNO₃ to remove any traces of carbonate from the solution. Aliquots of the Cr stock solution were added to separate polyethylene centrifuge tubes and diluted to 10 mL with deionized water that had been sparged with an inert gas to remove any trace of CO₂. Cr(OH)₃(am) was precipitated by adjusting the pH of the solution in each centrifuge tube to approximately 9.5 with CO₂-free NaOH. The precipitates were allowed to age overnight in the mother liquor, followed by washing three times with deionized water adjusted to pH 9.5 to reduce the concentration of soluble constituents, such as sodium and nitrate.

The washed precipitates were suspended in 35 mL of the NaOH or NaOH and NaNO₃ solutions of the appropriate molarity to prepare several sets for developing and testing the thermodynamic model (Table I). The suspensions thus prepared were placed on a shaker and continuously agitated and were sampled at different equilibration periods, as noted in Table I. Sampling consisted of centrifugation followed by filtration of the supernatant through (1) Amicon Type F-25 Centriflo Membrane Cones with 25,000 MW cutoff and approximately 0.0018- μ m pore size for suspensions containing < 1 *M* NaOH, (2) discs cut from the Amicon Type F-25 Centriflo Membrane Cones to fit a syringe filtration system, or (3) 0.22- μ m pore size Gelman nylon filters. Rai *et al.*⁽¹⁴⁾ describe the filtration procedure in detail, especially for 0.0018- μ m filters, and present data demonstrating the effectiveness of these filters in separating solids from solutions in the case of dissolved Cr species. A portion of the filtrate from selected samples was used to determine the oxidation states of aqueous Cr using the absorptive stripping voltammetry procedure described by Olsen *et al.*,⁽¹⁸⁾ where 0.05 *M* diethylenetriaminepentaacetic acid is used as a supporting electrolyte to measure Cr(VI) concentrations and where

Table I. Experimental Conditions for Different Sample Sets Used in Developing and Testing the Model

Set number (no. of samples)	Medium	Equilibration period (days)	Comments
Set I (8)	0.01 <i>m</i> NaClO ₄ 0.003 to 3.2 <i>m</i> NaOH	63, 134	Data of Rai <i>et al.</i> ^a
Set II	0.1 to 10.5 <i>m</i> NaOH	73, 151	0.0018- μ m Filtrates
Set III (6)	0.2 to 8.4 <i>m</i> NaOH	23	0.0018- μ m Filtrates
Set IV (16)	0.4 to 8.0 <i>m</i> NaOH	17, 98, 166	0.22- μ m Filtrates
Set V (10)	3.0 <i>m</i> NaOH, 0.1–7.5 <i>m</i> NaNO ₃	24, 39, 135	0.0018- μ m Filtrates
Set VI (7)	4.6 <i>m</i> NaNO ₃ , 0.1–3.5 <i>m</i> NaOH	22, 39, 137	0.0018- μ m Filtrates
Tank sludges (14)	Complex solutions containing 0.3–4.0 <i>m</i> OH		For details see Rapko <i>et al.</i> ^b and Lumetta <i>et al.</i> ^c

^aRef. 14.^bRef. 4.^cRefs. 5 and 6.

total Cr with this method is quantified by adding 0.001 *M* KMnO₄ to the sample to convert all Cr to Cr(VI). The filtrates for total Cr analyses were acidified to pH less than 1 to prevent the precipitation of Cr(OH)₃(am). The dissolved Cr concentrations in acidified filtrates were determined by a combination of techniques involving inductively coupled plasma emission spectroscopy (ICP) or inductively coupled plasma mass spectrometry (ICP-MS). The input molarities of NaOH or NaOH plus NaNO₃ solutions were converted to molality units using the solution density data reported in Weast⁽¹⁹⁾ and were used in modeling calculations because only a negligible fraction of hydroxide appeared to have been consumed in dissolution reactions (see results and discussion section for details). The information about the molarities and molalities of the bulk electrolyte solutions was used to convert Cr concentrations from molarity to molality units. All of the solubility data are reported in the Appendix in Tables AI–III.

X-ray diffraction (XRD) analyses were performed on selected equilibrated Cr precipitates. All precipitates were found to be amorphous to X rays. As a result, the solubility data reported in this study refer to the equilibrium solid phase as Cr(OH)₃(am).

Six precipitate and solution samples spanning the NaOH range from 0.2 to 8.4 *m* were selected for X-ray absorption spectroscopy (XAS) experiments. In addition, the XAS spectrum of a pH 2 aqueous solution was measured. The XAS experiments were conducted at the Stanford Synchrotron Radiation Laboratory (beamline 4 to 1). Spectra were collected at the Cr K-edge in fluorescence mode using a 13-element Ge detector. All precipitate samples were measured to photoelectron wavevector of 13 Å⁻¹. The solution samples were measured to

photoelectron wavevector of 10 \AA^{-1} due to the low Cr concentration. Energy calibration was based on assigning the first inflection point of the absorption edge of a Cr foil standard to 5989 eV. The absorption spectra were normalized by fitting polynomials through the pre- and postedge regions, setting the value of the extrapolated pre-edge to zero at E_0 , defined as 6000 eV for Cr. The difference between the extrapolations of the pre- and postedge polynomials was set to unity at E_0 . X-ray absorption fine structures (EXAFS) were extracted following standard procedures.⁽²⁰⁾ The EXAFS spectra of the Cr(III) precipitates and aqueous samples from precipitates equilibrated with 5.1 and 8.4 *m* NaOH were fit using parameterized phase and amplitude functions generated by FEFF7.0 using grimaldite (α -CrOOH)⁽²¹⁾ and guyanaite (β -CrOOH)⁽²²⁾ as structural models for the Cr–O and Cr–Cr scattering interactions.

2.1. Thermodynamic Model

The ion–interaction model of Pitzer and co-workers^(23,24) was used to interpret the solubility data. This aqueous thermodynamic model emphasizes a detailed description of specific ion interactions in solution. The effects of specific ion interactions on the excess solution free energy are contained in the expressions for the activity coefficients. The activity coefficients can be expressed in a virial-type expansion as

$$\ln \gamma_i = \ln \gamma_i^{\text{DH}} + \sum_j \beta_{ij}(I)m_j + \sum_j \sum_k C_{ijk}m_jm_k + \dots \quad (1)$$

where m_i is the molality of component i , γ_i^{DH} is a modified Debye–Hückel activity coefficient, which is a universal function of ionic strength, and $\beta_{ij}(I)$ and C_{ijk} are specific for each ion interaction and are functions of ionic strength. The third virial coefficient C is understood to be independent of ionic strength. A detailed description of the exact form of Eq. (1) is published in Felmy and Weare⁽²⁵⁾ and Felmy *et al.*⁽²⁶⁾ and is contained in the nonlinear least-squares programs (NONLIN and INSIGHT)⁽²⁷⁾ for estimating the activity coefficients and calculating chemical equilibria involving multiple solid and aqueous species. We have used these programs extensively in the past to interpret data for many systems extending to high ionic strengths and base concentrations^(26,28,29) similar to those investigated in this study.

3. RESULTS AND DISCUSSION

Dramatic increases are observed in aqueous Cr concentrations from Cr(OH)₃ (am) suspensions in NaOH with and without the presence of 4.6 *m* NaNO₃ (Figs. 1 and 2). Significant increases in aqueous Cr concentrations are also observed as a

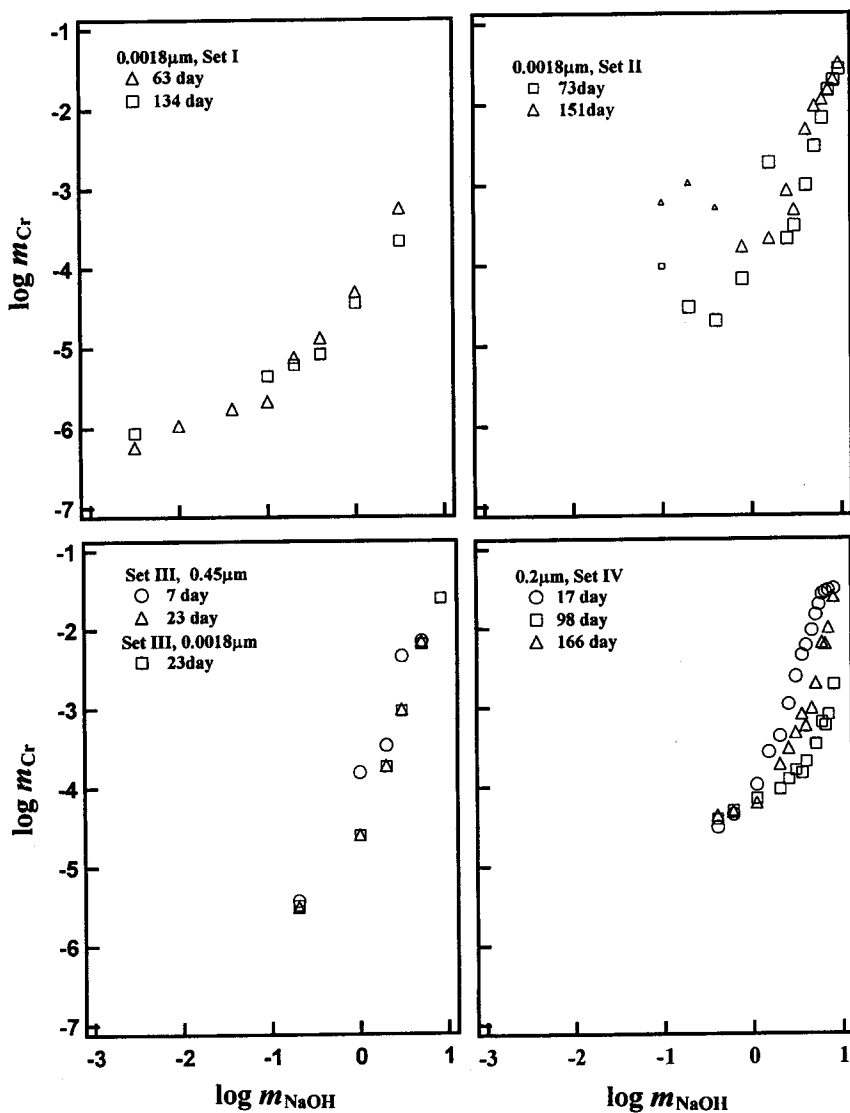


Fig. 1. Aqueous chromium concentrations from $\text{Cr}(\text{OH})_3(\text{am})$ suspensions in NaOH . Set I data are from Rai *et al.* (Ref. 14). Smaller symbols represent outliers.

function of high NaNO_3 concentrations containing 3.0 m NaOH (Fig. 3). The observed Cr concentrations at different equilibration periods for four out of six sets (Set I–III, Fig. 1; Fig. 2) show that steady-state concentrations appeared to have been reached between about 23 and 151 days. Two different sets (Set IV,

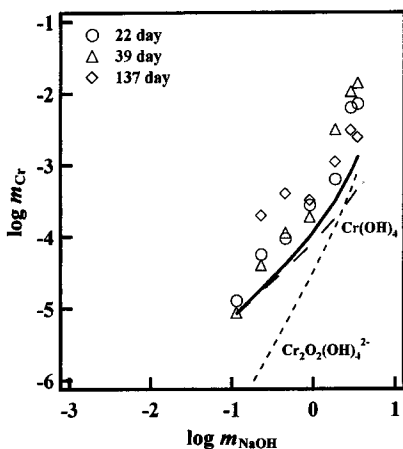


Fig. 2. Aqueous chromium concentrations from $Cr(OH)_3(am)$ suspensions in 4.6 *m* $NaNO_3$ containing different concentrations of $NaOH$ as noted in the figure. The solid line represents predicted total chromium concentrations; dashed lines represent the predicted concentrations of different species using thermodynamic data reported in Table IV.

Fig. 1; Fig. 3) indicate lower concentrations at longer equilibration periods. The reasons for these differences are not known. However, the observed variability in Cr concentrations in different sets as a function of time, in most cases, is less than an order of magnitude, whereas observed Cr concentrations increased by about five orders of magnitude with the increase in $NaOH$ concentrations from 0.1 to 10 *m*. Considering the difficulties involved in conducting these studies (*e.g.*, uncertainties in the use of filters of lowest pore diameters because of high ionic strengths and corrosive nature of the solutions and difficulties involved in analyzing these concentrated solutions reaching as high as 10 *m*) and that different $NaOH$ sets (Fig. 1) were executed under different conditions, by different individuals,

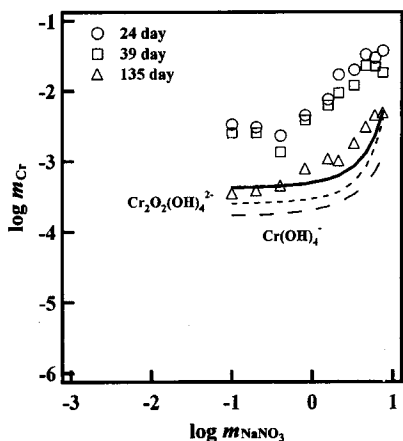


Fig. 3. Aqueous chromium concentrations from $Cr(OH)_3(am)$ suspensions in 3.0 *m* $NaOH$ containing different concentrations of $NaNO_3$ as noted in the figure. The solid line represents predicted total chromium concentrations; dashed lines represent the predicted concentrations of different species using thermodynamic data reported in Table IV.

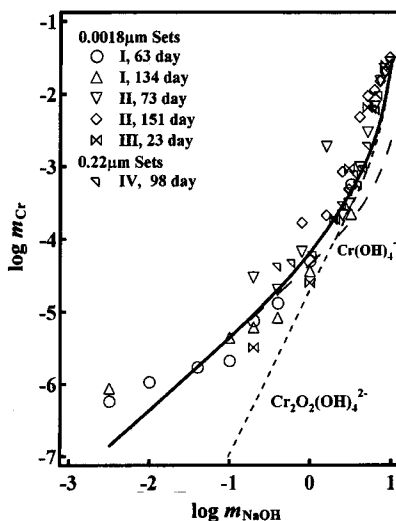


Fig. 4. Aqueous chromium concentrations from $\text{Cr}(\text{OH})_3(\text{am})$ suspensions in NaOH for 23- to 151-day equilibrations of different Sets, ignoring five data points from Set II that were clearly outliers. Lines represent predicted concentrations using the thermodynamic data developed in this study (Table IV); the solid line represents total chromium concentrations; other lines represent concentrations of different species as marked in the figure.

and in different laboratories, the degree of agreement among the different sets is remarkable (Fig. 4). Also, accepting the scatter and, as discussed later, the model developed from the NaOH system alone provides reasonable agreement with the observed concentrations from the concentrated $\text{NaNO}_3 + \text{NaOH}$ systems extending to as high ionic strengths as 10.5 *m* and NaNO_3 concentrations as high as 7.5 *m*. In addition, the equilibrium constant for the formation of $\text{Cr}(\text{OH})_4^-$ required to fit these data (presented later) is similar to that recently reported by Ziemniak *et al.*⁽¹⁵⁾ from a different system. These data collectively suggest that the chemical potential of the solid phase is reasonably constant over a period of about 23 to 151 days and thus reasonable values of equilibrium constants can be calculated from these data.

In addition to the data presented above, information on the dominant oxidation state of Cr is required to develop a reliable thermodynamic model from these data. Oxidation state analyses of many selected samples representative of different chemical systems involving $\text{Cr}(\text{OH})_3(\text{am})$ solubility in NaOH or in NaOH plus NaNO_3 (Sets II, V, and VI) were performed by absorptive stripping voltammetric analyses⁽¹⁸⁾ and by X-ray absorption near-edge structure (XANES) of a few samples. The stripping analyses showed that the dominant aqueous Cr oxidation state in all of these systems is Cr(III); the percentage of Cr(VI) in all cases was <18 and in most cases <4 (Table II). The background-subtracted, normalized XANES spectra for both the solution and precipitate samples (Fig. 5) display a profile that is consistent with the Cr(III) oxidation state. The XANES profile of Cr(VI) oxidation state is characterized by an intense pre-edge feature approximately 15 eV lower in energy than the main absorption edge. This pre-edge feature is not observed in any

Table II. Percent Cr(VI) in 0.0018- μm Filtrates from $\text{Cr}(\text{OH})_3(\text{am})$ Suspensions in Different Solutions

$\log m_{\text{NaOH}}$	$\log m_{\text{NaNO}_3}$	% Cr(VI)
Set II, 45 days		
0.200	0.000	1.8
0.400	0.000	9.2
0.800	0.000	17.4
1.600	0.000	15.7
2.508	0.000	9.0
3.015	0.000	10.2
4.040	0.000	2.1
5.084	0.000	1.6
6.151	0.000	1.2
7.248	0.000	0.1
8.379	0.000	0.6
9.551	0.000	0.3
10.447	0.000	0.4
Set V, 24 days		
3.015	0.101	1.5
3.015	0.202	3.6
3.015	0.406	3.0
3.015	0.821	2.1
3.015	1.574	1.5
3.015	2.134	0.7
3.015	3.319	1.1
3.015	4.602	0.4
3.015	5.998	1.2
3.015	7.523	1.1
Set VI, 22 days		
0.115	4.602	9.2
0.230	4.602	9.7
0.460	4.602	13.6
0.920	4.602	5.4
1.841	4.602	2.7
2.885	4.602	0.8
3.469	4.602	0.7

of the XANES profiles for the Cr samples, indicating that little, if any, Cr(VI) is present in these samples. The combination of both the stripping and XANES analyses show that the total observed Cr concentrations can be assumed to represent Cr(III) concentrations.

As discussed above, the chemical potential of the solid phase appears to be relatively constant over an equilibration period of about 23 to 151 days. In addition, the EXAFS analyses of the equilibrated solid phases from a large range in NaOH concentrations (0.2–8.4 m), discussed below, indicate that the nature of the solid

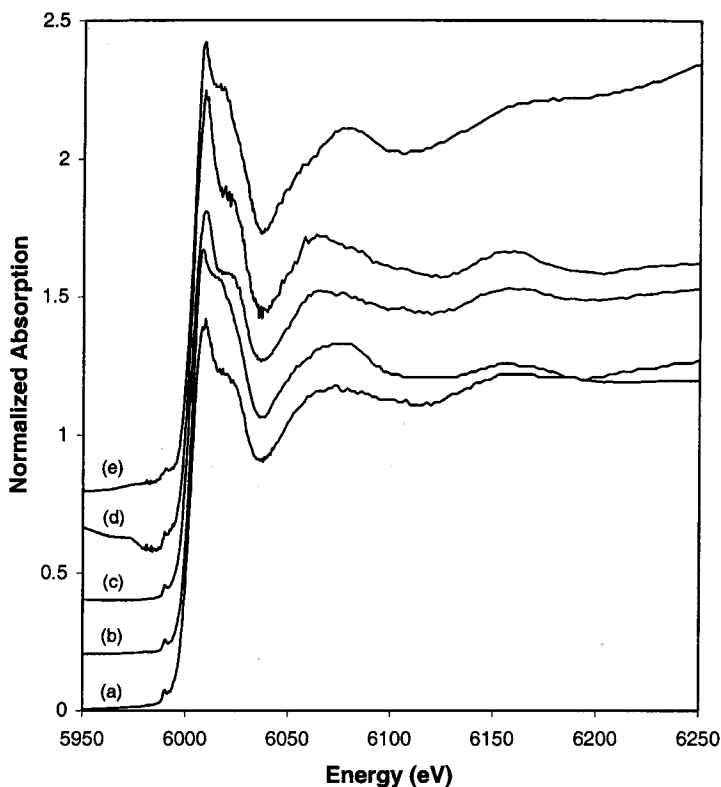


Fig. 5. Chromium K-edge XANES of both the aqueous solutions and solid precipitates in equilibrium with NaOH: (a) 0.2 *m* NaOH, solid precipitate; (b) 2.0 *m* NaOH, solid precipitate; (c) 5.1 *m* NaOH, solid precipitate; (d) 5.1 *m* NaOH, aqueous solution; and (e) pH 2.0, aqueous solution.

phases are similar in both the dilute and concentrated NaOH solutions. Thus the solubility-controlling solid phase in our entire study must be the same and most likely is $\text{Cr}(\text{OH})_3(\text{am})$. This agrees with results reported by Rai *et al.*⁽¹⁴⁾ for solutions at $\text{pH} < 14$ containing NaOH where the $\text{Cr}(\text{OH})_3(\text{am})$ prepared in a similar fashion was shown to reach equilibrium from both the over- and undersaturation directions within 6–63 days. For these reasons, the solubility data from 23 to 151 days equilibration were selected for developing the thermodynamic model (Fig. 4) for the solubility of $\text{Cr}(\text{OH})_3(\text{am})$.

The $\text{Cr}(\text{OH})_3(\text{am})$ solubility in NaOH (Fig. 4) shows a consistent trend of increasing solubility with increasing NaOH concentration, even to 10.5 *m* NaOH. This result is important because it indicates that significant amounts of Cr(III) can be solubilized at high NaOH concentrations, depending upon the type of

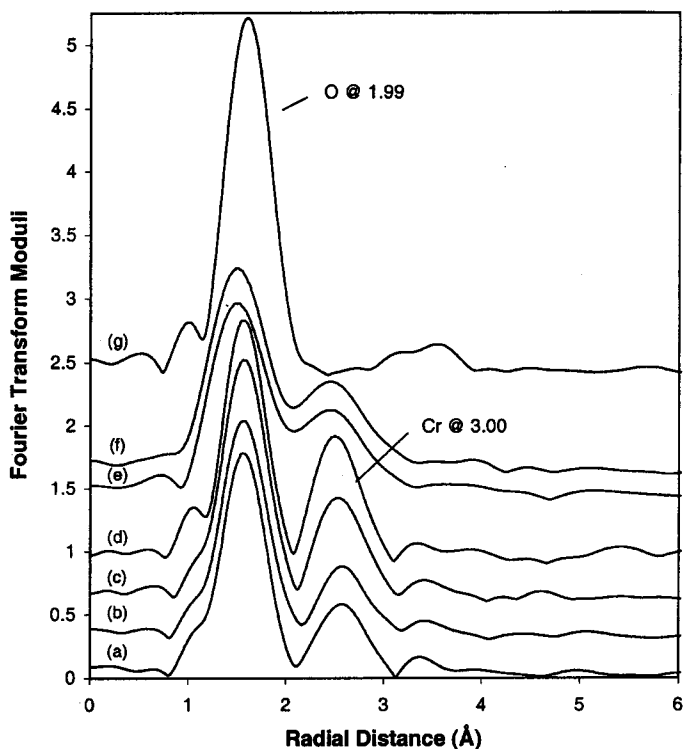


Fig. 6. Fourier transform of chromium K-edge EXAFS of both the aqueous solution and solid precipitate in equilibrium with NaOH: (a) 0.2 *m* NaOH, solid precipitate; (b) 2.0 *m* NaOH, solid precipitate; (c) 5.1 *m* NaOH, solid precipitate; (d) 8.4 *m* NaOH, solid precipitate; (e) 5.1 *m* NaOH aqueous solution; (f) 8.4 *m* NaOH, aqueous solution; and (g) pH 2.0, aqueous solution. The plotted residual distance is approximately 0.5 Å shorter than the actual interatomic distance because the phase shift is not removed.

solubility-controlling solid. The solubilities obtained in this study are also in close agreement with those of Rai *et al.*⁽¹⁴⁾ Two different techniques, EXAFS and thermodynamic analyses of solubility data, were used to identify the aqueous species. Fourier transforms of the extracted EXAFS are displayed in Fig. 6. The most intense peak corresponds to the Cr nearest-neighbor shell consisting of oxygen atoms. The second most prominent peak corresponds to the Cr next-nearest shell that consists of Cr atoms. Fits to the EXAFS of both the precipitates and basic aqueous solutions indicate that there are six nearest-neighbor oxygen atoms with 2.0 Å bonds to the Cr atom (Table III). This coordination environment is typical⁽³⁰⁾ for Cr³⁺. The Cr—O bond length determined for the acidic aqueous solution is slightly shorter, 1.96 Å (Table III). The Cr—Cr interatomic distance for both the

Table III. EXAFS Fitting Results for Solid Phases and Aqueous Species from Cr(OH)₃(am) Suspensions in Different Solutions

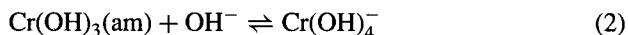
Solution	Parameter	Cr-O	Cr-Cr
Solid phases			
0.2 <i>m</i> NaOH	Distance	1.99 ± 0.01	3.00 ± 0.02
	Number	6.0 ± 1.4	1.5 ± 0.4
	Sigma	0.04 ± 0.02	0.06 ± 0.01
	δE ₀	3.2 ± 3.3	-4.8 ± 3.2
1.0 <i>m</i> NaOH	Distance	1.99 ± 0.02	2.99 ± 0.02
	Number	5.7 ± 1.3	1.8 ± 0.5
	Sigma	0.04 ± 0.02	0.06 ± 0.01
	δE ₀	3.4 ± 3.3	-5.7 ± 3.1
2.0 <i>m</i> NaOH	Distance	1.99 ± 0.02	3.00 ± 0.02
	Number	6.0 ± 1.4	1.6 ± 0.4
	Sigma	0.05 ± 0.02	0.06 ± 0.01
	δE ₀	3.1 ± 3.2	-4.0 ± 3.1
3.0 <i>m</i> NaOH	Distance	1.99 ± 0.02	2.99 ± 0.01
	Number	5.5 ± 1.2	1.4 ± 0.4
	Sigma	0.03 ± 0.02	0.04 ± 0.02
	δE ₀	2.8 ± 3.3	-4.6 ± 3.3
5.1 <i>m</i> NaOH	Distance	1.99 ± 0.01	2.98 ± 0.01
	Number	5.9 ± 1.3	2.2 ± 0.6
	Sigma	0.03 ± 0.02	0.06 ± 0.01
	δE ₀	3.9 ± 3.2	-4.2 ± 3.1
8.4 <i>m</i> NaOH	Distance	1.98 ± 0.02	2.95 ± 0.02
	Number	5.9 ± 1.6	1.9 ± 0.5
	Sigma	0.03 ± 0.01	0.04 ± 0.03
	δE ₀	2.5 ± 4.2	-4.2 ± 3.2
Aqueous species			
pH 2.0	Distance	1.96 ± 0.02	
	Number	7.6 ± 1.7	
	Sigma	0.02 ± 0.03	
	δE ₀	13.2 ± 3.3	
5.1 <i>m</i> NaOH	Distance	1.99 ± 0.02	2.96 ± 0.02
	Number	6.0 ± 1.3	2.7 ± 0.5
	Sigma	0.04 ± 0.02	0.07 ± 0.02
	δE ₀	3.2 ± 2.6	-7.4 ± 2.7
8.4 <i>m</i> NaOH	Distance	1.99 ± 0.02	2.95 ± 0.02
	Number	6.5 ± 1.4	2.6 ± 0.6
	Sigma	0.04 ± 0.02	0.06 ± 0.02
	δE ₀	4.0 ± 2.7	-6.6 ± 2.7

precipitates and basic aqueous solutions is determined to be approximately 3.0 Å, which is 0.9 Å shorter than expected for a linear Cr—O—Cr bond. However, the 3.0 Å interatomic distance corresponds to a bidentate bridge involving two oxygen atoms between the two Cr atoms that are found in both grimaldite (α -CrOOH)⁽²¹⁾

and guyanaite (β -CrOOH)⁽²²⁾ structures. There is no indication of Cr next-nearest neighbors for the acidic Cr aqueous solution. The fitting results to the EXAFS indicate that there is little or no change in the structure of the Cr precipitate as a function of NaOH concentration. In the 5.0 and 8.4 *m* NaOH aqueous solutions, where there is sufficiently high Cr concentration for EXAFS analysis, the Cr species is clearly polynuclear (Cr–Cr scattering path > 1). However, it is not possible to definitively determine whether the aqueous species is simply binuclear or a higher-order polymeric species. Polymeric Cr aqueous species with edge-sharing octahedral Cr³⁺ units have been previously observed at high Cr and NaCO₃ concentrations using EXAFS analysis.⁽³¹⁾ Our EXAFS analyses of aqueous Cr, although not definitive, were helpful in thermodynamic analyses of data presented in the next section.

3.1. Thermodynamic Analysis of Data

In our earlier work in dilute perchlorate media,⁽¹⁴⁾ we interpreted the Cr(OH)₃ (am) solubility data between pH 12 and 14 in terms of only one solubility reaction involving Cr(OH)₄[−] species⁵ with log K^0 equal to −4.3



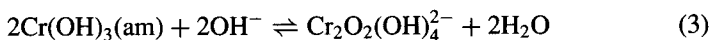
Because these data were in relatively dilute solution, the calculated standard-state equilibrium constant for this reaction should be reasonable. In fact, the estimated values of the formation constant for Cr(OH)₄[−] from these data⁽¹⁴⁾ are essentially identical to those recently reported by Ziemniak *et al.*⁽¹⁵⁾ from different chemical systems. However, it is not expected that this model would be valid at high NaOH concentration because of the large variation in the activity coefficients for OH[−] and Cr(OH)₄[−]. At high concentration, activity coefficients are not universal functions of ionic strength. This fact is accounted for in the Pitzer formalism by the use of ion–interaction coefficients for binary [*i.e.*, $\beta^{(0)}$ and $\beta^{(1)}$, C^ϕ for Na⁺–OH[−] and Na⁺–Cr(OH)₄[−]] and common-ion ternary interactions [*i.e.*, θ

⁵Because total Cr concentration is too low for EXAFS analysis where the Cr(OH)₄[−] species is dominant (Fig. 4 and Ref. 14), it was not possible to directly determine the Cr³⁺ coordination environment in Cr(OH)₄[−]. Furthermore, the concentration of Cr(OH)₄[−] is too low to detect these species either spectrophotometrically or by hydroxyl titration, contrary to the results published by Bradley *et al.* (Ref. 32). The existence of Cr(OH)₄[−] also not necessitate a tetrahedrally coordinated Cr³⁺ as implied by Bornholdt *et al.* (Ref. 31) and Bradley *et al.* (Ref. 32) because the Cr³⁺ in these species could be octahedrally coordinated with two additional oxygen atoms supplied by associated water molecules. Nevertheless, this change in the structural composition of Cr(OH)₄[−] would not require changes in the equilibrium constants of reactions involving this species. For these reasons, we choose to use Cr(OH)₄[−], which is consistent with Rai *et al.* (Ref. 14) and Ziemniak *et al.* (Ref. 15) and recommended by Ball and Nordstrom (Ref. 17), to model Cr(OH)₃(am) solubility in relatively low concentrations of NaOH.

for OH⁻-Cr(OH)₄⁻]. Although the necessary Pitzer ion-interaction parameters for Na⁺-OH⁻ are well known, the parameters involving the Cr(OH)₄⁻ ion are unknown and must be calculated (fit) or estimated. As an example, if the equilibrium reaction, Eq. (2), given by Rai *et al.*⁽¹⁴⁾ is combined with the Pitzer ion-interaction parameters⁽²⁴⁾ for Na⁺-OH⁻ and the values⁽³³⁾ for Al(OH)₄⁻-Na⁺ are used as analogs for Cr(OH)₄⁻-Na⁺, the predicted solubilities agree closely with the experimental data at low NaOH concentrations (<1 *m*), but are significantly below the experimental values at higher NaOH concentration (Fig. 4).

To interpret the data at high hydroxide concentrations, information regarding the concentrations and structures of the dominant Cr(III) species is needed. Although a number of species (monomer, dimer, trimer, and tetramer) have been identified under acidic conditions,⁽³⁴⁻³⁷⁾ structural formulas of only monomer and dimer have been identified with reasonable certainty.^(34,35,38) Unfortunately, with the exception of our EXAFS data showing that the Cr(III) species in >5.0 *M* NaOH are polymeric, no structural information is available on Cr(III) species in alkaline solutions. In the absence of such information, several attempts were made to explain the observed solubility behavior as a function of hydroxide concentrations. We based our explanation on the knowledge that log *m*_{Cr} vs. log *m*_{OH} has a slope of about unity in the low hydroxide concentration region and a slope of about 2.5 (Fig. 4) in the high hydroxide concentration region, and the realization that slopes are dependent on the aqueous species and their combinations and the associated ion-interaction parameters, especially in concentrated electrolytes as used in this study. In these attempts, we included different mononuclear and polynuclear species [Cr(OH)₅²⁻, Cr(OH)₆³⁻, Cr₂O₂(OH)₄²⁻, and Cr₃O₄(OH)₄³⁻], which (1) might provide slopes of 2 or 3 to account for the observed behavior in high hydroxide concentration regions or that (2) are postulated structures [*i.e.*, Cr₂O₂(OH)₄²⁻, and Cr₃O₄(OH)₄³⁻] that result from the conversion of hydroxo bridges in dimer [Cr₂(OH)₂(H₂O)₄⁴⁺] and trimer reported under acidic conditions to oxygen bridges through deprotonation/dehydration under higher concentrations of hydroxide, as pointed out by Hall and Eyring⁽³⁹⁾ and consistent with our EXAFS data, in conjunction with Cr(OH)₄⁻ species expected to be dominant in the low hydroxide concentration region. In addition to the fact that EXAFS indicates the existence of polynuclear species and that the presence of Cr(OH)₅²⁻ and Cr(OH)₆³⁻ would be inconsistent with these data, there are no data in the JCPDS for Cr(III) solid phases of higher sodium content than NaCrO₂(c). This indicates that structural units, such as Cr(OH)₅²⁻ or Cr(OH)₆³⁻, are not important, at least in the solid phases. These facts and the inability to account for all of the observed Cr(III) solubility behavior in thermodynamic analyses of the solubility data were used to eliminate Cr(OH)₅²⁻ and Cr(OH)₆³⁻ from consideration as important species in concentrated NaOH solutions. The final model that included a minimum number of species and showed close agreement between the observed and model-predicted Cr concentrations in NaOH systems extending to 10.5 *m*

included $\text{Cr}_2\text{O}_2(\text{OH})_4^{2-}$ and $\text{Cr}(\text{OH})_4^-$. Because $\text{Cr}_2\text{O}_2(\text{OH})_4^{2-}$ has a charge of 2 and the solutions range from low to very high NaOH concentrations, the ion–interaction parameters for $\text{Cr}_2\text{O}_2(\text{OH})_4^{2-}$ with Na^+ cannot be ignored. Because these parameters for $\text{Na}^+ - \text{Cr}_2\text{O}_2(\text{OH})_4^{2-}$ are not available, we assumed that the $\beta^{(0)}$ and $\beta^{(1)}$ values that we determined previously⁽²⁸⁾ for $\text{Cd}(\text{OH})_4^{2-}$, a divalent anion similar to $\text{Cr}_2\text{O}_2(\text{OH})_4^{2-}$, with Na^+ are applicable to this system. The use of these parameters provided a very close fit to the data up to about 5.0 *m* NaOH. However, this model underpredicted the Cr concentrations at >5.0 *m* NaOH. The extent of the underprediction reached about 0.4 log units at 10.5 *m* NaOH. To improve the modeling predictions in these concentrated NaOH solutions, the model was modified to include either (1) trimer $[\text{Cr}_3\text{O}_4(\text{OH})_4^{3-}]$ with associated binary ion–interaction parameters of this species, with Na^+ assumed to be identical to those for $\text{Na}^+ - \text{Nd}(\text{CO}_3)_3^{3-}$ (another trivalent anion, reported by Rao *et al.*⁽⁴⁰⁾), or (2) C^ϕ for $\text{Na}^+ - \text{Cr}_2\text{O}_2(\text{OH})_4^{2-}$, which provided almost identical calculated values that were in close agreement with the observed Cr concentrations at >5.0 *m* NaOH. However, because (1) the model containing C^ϕ for $\text{Na}^+ - \text{Cr}_2\text{O}_2(\text{OH})_4^{2-}$ is simpler (does not include additional species), (2) there is no objective reason to exclude C^ϕ in these concentrated solutions, and (3) the values of C^ϕ required to interpret the data are reasonable (discussed below), we have selected the model containing C^ϕ for interpretation of all of the data. It is possible, however, that a small percentage of polynuclear species higher than $\text{Cr}_2\text{O}_2(\text{OH})_4^{2-}$ may be present, especially in solutions of >5.0 *m* NaOH. Simultaneously fitting $\Delta G_f^0/RT$ for $\text{Cr}_2\text{O}_2(\text{OH})_4^{2-}$ and $\text{Cr}(\text{OH})_4^-$ and C^ϕ for $\text{Na}^+ - \text{Cr}_2\text{O}_2(\text{OH})_4^{2-}$ with the inclusion of other appropriate species and parameters provided a value of -0.03768 for C^ϕ , and $\log K^0$ values of -4.36 ± 0.24 and -5.24 ± 0.24 for $\text{Cr}(\text{OH})_3(\text{am})$ solubility reactions involving $\text{Cr}(\text{OH})_4^-$ (Eq. 2) and $\text{Cr}_2\text{O}_2(\text{OH})_4^{2-}$ (Eq. 3), respectively



The $\log K^0$ value for Eq. (2) obtained in this study, with the use of ion–interaction parameters, is essentially identical to that we determined previously⁽¹⁴⁾ without the inclusion of these parameters. No literature data are available for comparison with the values of the equilibrium constant that we determined for Eq. (3). The value of C^ϕ we determined for $\text{Na}^+ - \text{Cr}_2\text{O}_2(\text{OH})_4^{2-}$ is negative, as is the case with many other 2:1 electrolytes and is very similar in sign and magnitude to the C^ϕ values reported for several other 2:1 electrolytes [e.g., $\text{UO}_2(\text{NO}_3)_2$, UO_2Cl_2 , and CuCl_2].⁽²⁴⁾

The constants and ion–interaction parameters used in the final model are reported in Table IV. There is close agreement between the observed and predicted Cr concentrations in equilibrium with $\text{Cr}(\text{OH})_3(\text{am})$ in NaOH solutions ranging

Table IV. Pitzer Ion–Interaction Parameters and Thermodynamic Equilibrium Constants used in the Final Model

Species	Binary parameters				Reference
	$\beta^{(0)}$	$\beta^{(1)}$	$\beta^{(2)}$	C^ϕ	
H ⁺ –ClO ₄ [−]	0.1747	0.2931	0.00	0.00819	24
Na ⁺ –OH [−]	0.0864	0.253	0.00	0.0044	24
Na ⁺ –ClO ₄ [−]	0.0554	0.2755	0.00	−0.00118	24
Na ⁺ –Cr(OH) ₄ [−]	0.045	0.31	0.00	−0.003	This study ^a
Na ⁺ –NO ₃ [−]	0.0068	0.1783	0.00	−0.00072	24
Na ⁺ –Al(OH) ₄ [−]	0.045	0.31	0.00	−0.003	33
Na ⁺ –Cr ₂ O ₂ (OH) ₄ ^{2−}	0.41	0.7	0.00	−0.03768	This study ^b
Common-ion ternary parameters					
	Value				
OH [−] –Cr(OH) ₄ [−]	0.014				This study ^a
OH [−] –Cr(OH) ₄ [−] –Na ⁺	−0.0048				This study ^a
OH [−] –Al(OH) ₄ [−]	0.014				33
OH [−] –Al(OH) ₄ [−] –Na ⁺	−0.0048				33
H ⁺ –Na ⁺	0.036				24
Equilibrium constants					
Reaction	log K^0				
Cr(OH) ₃ (am) ⇌ Cr(OH) ₃	<−6.84				14
Cr(OH) ₃ (am) + OH [−] ⇌ Cr(OH) ₄ [−]	−4.36 ± 0.24				This study ^c
2Cr(OH) ₃ (am) + 2OH [−] ⇌ Cr ₂ O ₂ (OH) ₄ ^{2−} + 2H ₂ O	−5.24 ± 0.24				This study

^a Assumed to be identical to Na⁺–Al(OH)₄[−] parameters reported by Wesolowski (Ref. 33).

^b Values of $\beta^{(0)}$ and $\beta^{(1)}$ assumed to be identical to Cd(OH)₂^{2−}–Na⁺ reported by Rai *et al.* (Ref. 28) (see text for details).

^c The log K^0 value calculated in this study with the inclusion of ion–interaction parameters for Cr(OH)₄[−] is identical to that reported by Rai *et al.* (Ref. 14).

in concentrations from 0.003 to 10.5 *m*, indicating that the selected modeling parameters provide reliable predictions of the solubility behavior of Cr(OH)₃(am) over a wide range of hydroxide concentrations (Fig. 4). It is also of interest to determine how closely this model predicts the observed solubility behavior of Cr(OH)₃(am) in mixed systems containing 3 *m* NaOH and NaNO₃ varying from 0.1 to 7.5 *m*, or 4.6 *m* NaNO₃ and NaOH varying from 0.1 to 3.5 *m* NaOH. A reasonably close agreement between the observed and predicted concentrations indicates that our model is also consistent with the Cr(OH)₃(am) solubility in mixed NaOH–NaNO₃ systems, with no model parameters adjusted (Figs. 2 and 3). This latter fact is especially important, because it represents at least a partial validation of this thermodynamic model.

In summary, the solubility of $\text{Cr}(\text{OH})_3(\text{am})$ was studied in NaOH and mixed NaOH– NaNO_3 solutions extending to high concentration. The results at lower NaOH (*i.e.*, $<2\text{ m}$ NaOH) are consistent with our previous studies.⁽¹⁴⁾ A relatively simple thermodynamic model was developed that includes only two aqueous Cr species [$\text{Cr}_2\text{O}_2(\text{OH})_4^{2-}$ and $\text{Cr}(\text{OH})_4^-$] and explains all the solubility data for $\text{Cr}(\text{OH})_3(\text{am})$ in both NaOH and NaOH– NaNO_3 solutions extending to high electrolyte concentrations. This is the only Cr(III) thermodynamic data/model applicable to concentrated electrolytes, in general, and to hydroxide and nitrate, in particular, which are important in high-level nuclear wastes stored in tanks. A preliminary application of this model in predicting leachability of Cr from high-level tank sludges is discussed in the next section.

3.2. Modeling the Leachability of Chromium from High-Level Nuclear Waste Storage Tank Sludges

Although the fundamental model that we developed is relatively simple and is based only on studies for NaOH and mixtures of NaOH and NaNO_3 , it is of interest to determine the reliability and limitations of this model in predicting leachable Cr from actual high-level nuclear waste storage-tank sludges. Predicting Cr concentrations from tank sludges is complicated by many factors, including those that affect concentrations of Cr(III), such as (1) high ionic strength, (2) the presence of concentrated electrolytes containing nitrates, nitrites, aluminates, sodium, and, in some cases, elevated concentrations of carbonates, fluoride, and phosphate, and (3) the types of solubility-controlling Cr(III) solid phases. In addition, oxidation/reduction conditions and the presence of residual Cr(VI) in the tanks [*e.g.*, large amounts of Cr(VI) are reported in REDOX and TBP process wastes⁽⁸⁾] can change the proportion of soluble Cr(III) and Cr(VI) in tank supernates. This can impact our ability to compare predicted and observed concentrations, especially when relative concentrations of Cr(III) and Cr(VI) are not available, as is the case with many samples analyzed recently.^(4–6) These leaching experiments also present difficulties such as: (1) the concentrated NaOH solutions used may have contained soluble carbonates; (2) the solutions were either centrifuged and decanted or filtered through $0.45\text{-}\mu\text{m}$ filters; (3) the first caustic wash was sometimes preceded by a prewash and sometimes not, which could result in changes in solution concentrations of the equilibrated solutions [including the relative amounts of Cr(III) and Cr(VI)]; (4) data on the oxidation state distributions of Cr in leachates are lacking or extremely limited; (5) the concentrations of hydroxide in dilute NaOH prewashes were not analyzed; and (6) temperatures were variable and the gaseous atmosphere uncontrolled. As a result of expected changes in the number of variables from tank to tank and in different wash sequences (prewash and first and second caustic washes), we expect that our model, in general, should agree more

closely with observed concentrations as the wash sequence proceeds from pre-wash to first caustic wash to second caustic leach, because the overall system approaches the condition of leaching the $\text{Cr}(\text{III})$ solids from sludges with almost pure NaOH .

Results from first and second caustic leachates from solids from 14 different Hanford tanks containing wastes representative of the four major chemical processing operations (REDOX, TBP, BiPO_4 , and PUREX) were selected for

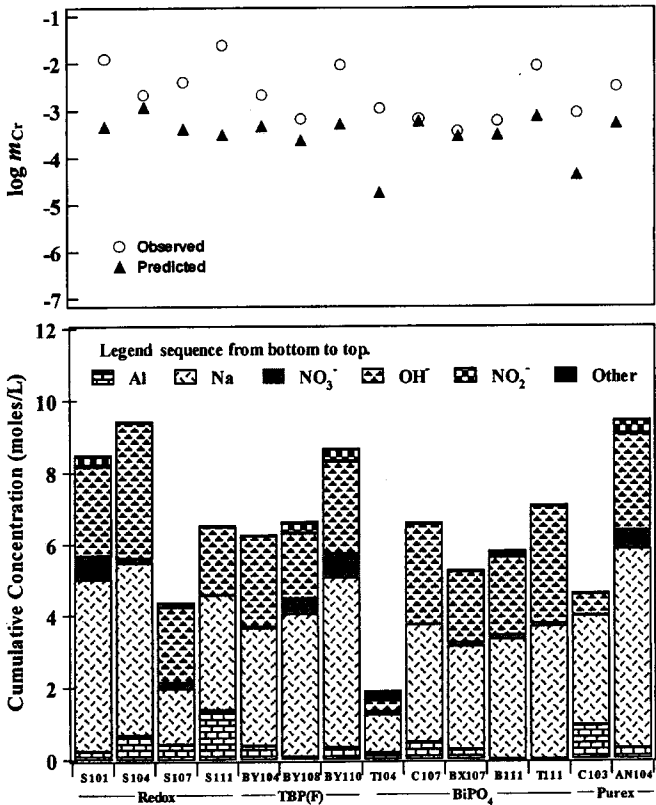


Fig. 7. Aqueous concentrations of major constituents (other refers to phosphate and sulfate) in first caustic wash of solids from different tanks that received different types of processing wastes (bottom graph). The top graph compares soluble chromium concentrations predicted using the chemical compositions of caustic washes and the thermodynamic data in Table IV and observed concentrations in first caustic washes of different tanks. All experimental data from Rapko *et al.* (Ref. 4) and Lumetta *et al.* (Refs. 5, 6).

comparing observed⁽⁴⁻⁶⁾ with predicted Cr concentrations using our model (Table IV). Observations based on concentrations of leachates from these tanks (Figs. 7 and 8) indicate: (1) both the first and second leachates contain relatively high total electrolyte concentrations reaching as high as 10 M and, on average, contain about 6 M; (2) the first caustic leach contains significant, but variable, concentrations of Al, Na, nitrate, hydroxide, and nitrite; and (3) the second caustic leach primarily contains Na and hydroxide, with a few of the tanks containing

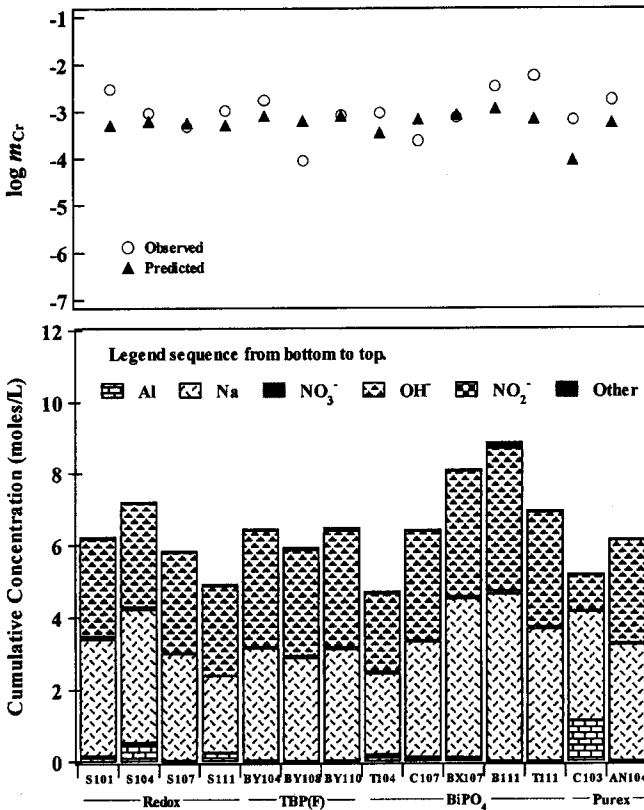


Fig. 8. Aqueous concentrations of major constituents (other refers to phosphate and sulfate) in second caustic wash of solids from different tanks that received different types of processing wastes (bottom graph). Top graph compares soluble chromium concentrations predicted using the chemical compositions of caustic washes and the thermodynamic data in Table IV and observed concentrations in second caustic washes of different tanks. All experimental data from Rapko *et al.* (Ref. 4) and Lumetta *et al.* (Refs. 5, 6).

significant concentrations of Al (*e.g.*, Tanks S104 and C103; Fig. 8). Our predicted Cr concentrations are, on average, about 0.9 ± 0.6 orders of magnitude lower than the observed Cr concentrations for the first caustic leach for most waste types⁶ (Fig. 7). The reason for the underprediction is not known, but we believe it is not related to our selection of the solubility-controlling solid phase, because the Cr(OH)₃(am) selected for modeling is the most soluble of the Cr(III) solid phases expected to be present in tank sludges. We surmise it may have to do with a combination of factors involving the presence of Cr(VI), procedures used in sludge washing, and the presence of significant concentrations of electrolytes other than NaOH, which, at present, are not included in our model. For the second alkaline wash, our predicted Cr concentrations are in excellent agreement with observed Cr concentrations (Fig. 8). This close agreement suggests that the solubility-controlling phases in these tank leachates must be Cr(OH)₃(am) and, further, that soluble levels of Cr must either be Cr(III) or controlled by the solubility of Cr(OH)₃(am).

APPENDIX

Complete data for Cr(OH)₃(am) solubility in different solutions presented in Figs. 1–3, 5, and 7 are reported in Tables AI–III.

Table AI. Chromium Concentrations in 0.0018- μ m Filtrates from Cr(OH)₃(am) Suspensions in 0.01 M NaClO₄ Containing Different Concentrations of NaOH Equilibrated for Different Periods^a

m_{NaOH}	$\log m_{\text{Cr}}$	
	63 Days	134 Days
Set I		
0.003	-6.239	-6.058
0.010	-5.968	ND ^b
0.040	-5.762	ND ^b
0.100	-5.675	-5.354
0.200	-5.125	-5.211
0.400	-4.877	-5.083
1.000	-4.304	-4.442
3.178	-3.253	-3.657

^aRef. 14.

^bND, below detection.

⁶They are about three orders of magnitude lower for retrieval and dilute NaOH washes (data not presented).

Table AII. Chromium Concentrations in Filtrates from $\text{Cr}(\text{OH})_3(\text{am})$ Suspensions in Different Concentrations of NaOH Equilibrated for Different Periods

m_{NaNO_3}	$\log m_{\text{Cr}}$		
Set II	45 Days ^a	73 Days ^a	151 Days ^a
0.100	-5.838	-4.022	-3.215
0.200	-4.128	-4.527	-2.977
0.400	-4.449	-4.696	-3.294
0.800	-4.464	-4.180	-3.777
1.600	-3.984	-2.732	-3.684
2.508	-3.328	-3.685	-3.078
3.015	-2.985	-3.523	-3.323
4.040	-2.420	-3.015	-2.322
5.084	-2.020	-2.533	-2.033
6.151	-1.714	-2.182	-1.951
7.248	-1.493	-1.825	-1.834
8.379	-1.183	-1.709	-1.696
9.551	-1.122	-1.566	-1.495
10.447	-1.097	-1.291	-1.838
Set III	7 Days ^b	23 Days ^a	23 Days ^b
0.200	-5.430	-5.488	-5.512
1.000	-3.809	-4.596	-4.597
2.003	-3.468	-3.738	-3.732
3.015	-2.336	-3.030	-3.022
5.084	-2.150	-2.190	-2.163
8.379	ND ^c	-1.606	ND ^c
Set IV	17 Days ^d	98 Days ^d	166 Days ^d
0.400	-4.512	-4.370	-4.411
0.600	-4.354	-4.323	-4.304
1.100	-3.984	-4.214	-4.158
1.500	-3.567	ND ^c	ND ^c
2.003	-3.373	-3.729	-4.041
2.508	-2.968	-3.533	-3.916
3.015	-2.620	-3.335	-3.799
3.526	-2.351	-3.100	-3.841
3.937	-2.232	-3.249	-3.695
4.559	-2.043	-3.029	ND ^c
5.084	-1.844	-2.709	-3.478
5.508	-1.715	ND ^c	ND ^c
5.935	-1.576	-2.201	-3.204
6.477	-1.549	-2.213	-3.242
7.026	-1.526	-2.012	-3.106
8.036	-1.510	-1.622	-2.723

^aFiltered through 0.0018 μm .

^bFiltered through 0.45 μm .

^cND, no data.

^dFiltered through 0.22 μm .

Table AIII. Chromium Concentrations in 0.0018- μm Filtrates from Cr(OH)₃(am) Suspensions in NaOH Containing Different Concentrations of NaNO₃ Equilibrated for Different Periods

m_{NaOH}	m_{NaNO_3}	$\log m_{\text{Cr}}$		
Set V		24 Days	39 Days	135 Days
3.015	0.101	-2.476	-2.605	-3.459
3.015	0.202	-2.516	-2.599	-3.376
3.015	0.406	-2.643	-2.874	-3.297
3.015	0.821	-2.349	-2.424	-3.055
3.015	1.574	-2.116	-2.211	-2.922
3.015	2.134	-1.772	-2.030	-2.953
3.015	3.319	-1.701	-1.918	-2.700
3.015	4.602	-1.482	-1.641	-2.475
3.015	5.998	-1.526	-1.652	-2.330
3.015	7.523	-1.428	-1.736	-2.291
Set VI		22 Days	39 Days	137 Days
0.115	4.602	-4.887	-5.055	
0.230	4.602	-4.246	-4.402	-3.710
0.460	4.602	-4.025	-3.947	-3.397
0.920	4.602	-3.562	-3.732	-3.494
1.841	4.602	-3.198	-2.506	-2.959
2.885	4.602	-2.197	-1.979	-2.515
3.469	4.602	-2.149	-1.858	-2.625

ACKNOWLEDGMENTS

This research was conducted at the Pacific Northwest National Laboratory (operated by Battelle for the U.S. Department of Energy (DOE) under contract DE-AC06-76RL01830), Lawrence Berkeley National Laboratory (under U.S. Department of Energy Contract No. DE-AC03-76SF00098), and Washington State University. X-ray absorption spectroscopy experiments were conducted at the Stanford Synchrotron Radiation Laboratory, operated by the U.S. Department of Energy, Office of Basic Energy Sciences. The research was funded by the DOE under the Environmental Management Sciences Program (65368). We thank Khri Olsen and Robert Fulton for analytical help, Kathi Hanson for editorial support, and Debra M. Hinton for help with text processing of this document (ms 3449 with Sludge Data 419.doc).

REFERENCES

1. P. Hrma, J. Vienna, J. Crum, G. Piepel, and M. Mika, *Mater. Res. Soc. Proc.* **608**, 671 (2000).
2. J. L. Swanson, *Clean Option: An Alternative Strategy for Hanford Tank Waste Remediation. Volume 2: Detailed Description of First Example Flowsheet*, PNL-8288, Vol 2 (Pacific Northwest National Laboratory, Richland, Washington, 1993).

3. G. J. Lumetta and B. M. Rapko, *Separation Sci. Technol.* **34**, 1495 (1999).
4. B. M. Rapko, G. J. Lumetta, and M. J. Wagnor, *Washing and Caustic Leaching of Hanford Tank Sludges: Results of FY 1995 Studies*, PNL-10712 (Pacific Northwest National Laboratory, Richland, Washington, 1995).
5. G. J. Lumetta, B. M. Rapko, M. J. Wagner, J. Liu, and Y. L. Chen, *Washing and Caustic Leaching of Hanford Tank Sludge: Results of FY 1996 Studies*, PNNL-11278, Rev. 1 (Pacific Northwest National Laboratory, Richland, Washington, 1996).
6. G. J. Lumetta, I. E. Burgeson, M. J. Wagnor, J. Liu, and Y. L. Chen, *Washing and Caustic Leaching of Hanford Tank Sludge: Results of FY 1997 Studies*, PNNL-11636 (Pacific Northwest National Laboratory, Richland, Washington, 1997).
7. M. J. Kupfer, A. L. Boldt, K. M. Hodgson, L. W. Shelton, B. C. Simpson, R. A. Watrous, B. A. Higley, R. M. Orme, M. D. LeClair, G. L. Borsheim, R. T. Winward, N. G. Colton, S. L. Lambert, D. E. Place, and W. W. Schultz, *Standard Inventories of Chemicals and Radionuclides in Hanford Site Tanks*, HNF-SD-WM-TI-740, Rev 0B (Lockheed Martin Hanford Company, Richland, Washington, 1998).
8. D. L. Blanchard, S. D. Conradson, N. J. Hess, and P. K. Melethil, *Sludge Component Speciation: Summary Final Report*, TWRSP-95-048 (Pacific Northwest National Laboratory, Richland, Washington, 1995).
9. J. D. Anderson, *A History of the 200 Area Tank Farms*, WHC-MR0132 (Westinghouse Hanford Company, Richland, Washington, 1990).
10. N. G. Colton, *Status Report: Pretreatment Chemistry Evaluation FY1997—Wash and Leach Factors for the Single-Shell Waste Inventory*, PNNL-11646 (Pacific Northwest National Laboratory, Richland, Washington, 1997).
11. D. Rai and J. M. Zachara, *Sci. Total Environ.* **86**, 15 (1989).
12. J. P. LaFemina, *Tank Waste Treatment Science Task Quarterly Report for April–June 1995*, PNL-10764 (Pacific Northwest National Laboratory, Richland, Washington 1995).
13. R. Fricke, and O. Windhausen, *Z. Anorg. Allgem. Chem.* **132**, 273 (1924).
14. D. Rai, B. M. Sass, and D. A. Moore, *Inorg. Chem.* **26**, 345 (1987).
15. S. E. Ziemniak, M. E. Jones, and K. E. S. Combs, *J. Solution Chem.* **27**, 33 (1998).
16. von U. von Meyenburg, O. Sirok, and G. Schwarzenbach, *Helv. Chim. Acta* **56**, 1099 (1973).
17. J. W. Ball, and D. K. Nordstrom, *J. Chem. Eng. Data* **43**, 895 (1998).
18. K. B. Olsen, J. Wang, R. Setiadjji, and J. Lu, *Environ. Sci. Technol.* **28**, 2074 (1994).
19. R. C. Weast, *Handbook of Chemistry and Physics* (CRC Press, Boca Raton, FL Ohio FL 1972–1973).
20. B. K. Teo, *EXAFS: Basic Principles and Data Analyses, Inorganic Chemistry Concepts 9* (Springer-Verlag, New York, 1986).
21. A. N. Christensen, P. Hansen, and M. S. Lehmann, *J. Solid State Chem.* **21**, 325 (1977).
22. A. N. Christensen, P. Hansen, and M. S. Lehmann, *J. Solid State Chem.* **19**, 299 (1976).
23. K. S. Pitzer and G. Mayorga, *J. Phys. Chem.* **77**, 2300 (1973).
24. K. S. Pitzer, *Ion Interaction Approach: Theory and Data Correlation* (CRC Press, Boca Raton, FL, 1991), Chap. 3.
25. A. R. Felmy and J. H. Weare, *Geochim. Cosmochim. Acta* **50**, 2771 (1986).
26. A. R. Felmy, D. Rai, J. A. Schramke, and J. L. Ryan, *Radiochim. Acta* **48**, 29 (1989).
27. S. M. Sterner, A. R. Felmy, J. R. Rustad, and K. S. Pitzer, *Thermodynamic Analysis of Aqueous Solutions Using INSIGHT*, PNWD-SA-4436 (Pacific Northwest National Laboratory, Richland, Washington, 1997).
28. D. Rai, A. R. Felmy, and R. W. Szelmezcza, *J. Solution Chem.* **20**, 375 (1991).
29. D. Rai, A. R. Felmy, S. M. Sterner, D. A. Moore, and M. J. Mason, *Radiochim. Acta* **79**, 239 (1997).

30. J. R. Smyth and D. L. Bish, *Crystal Structures and Cation Sites of the Rock-Forming Minerals* (Allen and Unwin, Boston, MA, 1988).
31. K. Bornholdt, J. M. Corker, J. Evans, and J. M. Rummey, *Inorg. Chem.* **30**, 1 (1991).
32. S. M. Bradley, C. R. Lehr, and R. A. Kydd, *J. Chem. Soc. Dalton Trans.*, p. 2415 (1993).
33. D. J. Wesolowski, *Geochim. Cosmochim. Acta* **56**, 1065 (1992).
34. L. A. Laswick and R. A. Plane, *J. Amer. Chem. Soc.* **81**, 3564 (1959).
35. R. W. Kolaczowski and R. A. Plane, *Inorg. Chem.* **3**, 322 (1964).
36. J. E. Finholt, M. E. Thompson, and R. E. Connick, *Inorg. Chem.* **20**, 4151 (1981).
37. H. Stunzi, L. Spiccia, F. P. Rogzinger, and W. Marty, *Inorg. Chem.* **28**, 66 (1989).
38. M. Thompson and R. E. Connick, *Inorg. Chem.* **20**, 2279 (1981).
39. H. T. Hall and H. Eyring, *J. Amer. Chem. Soc.* **72**, 782 (1950).
40. L. Rao, D. Rai, A. R. Felmy, R. W. Fulton, and C. F. Novak, *Radiochim. Acta* **75**, 141 (1996).